Journal of
Vibration and Control

Experimental Bifurcation Control of a Parametric Pendulum

SCHOLARONE™
Manuscripts

1
2
3
4
5
6
7
8
9
10
11
12
13
14
15
16
17
18
19
20
21
22
23
24
25
26
27
28
29
30
31
32
33
34
35
36
37
38
39
40
41
42
43
44
45
46
47
48
49
50
51
52
53
54
55
56
57
58
59
60

104x30mm (300 x 300 DPI)

Experimental Bifurcation Control of a Parametric Pendulum

Aline S. De Paula[1], Marcelo A. Savi[2], S. Vahid Vaziri H.[3], Ekaterina Pavlovskaia[3] and Marian Wiercigroch[3]

Abstract

The aim of the study is to maintain the desired period-1 rotation of the parametric pendulum over a wide range of the excitation parameters. Here the Time-Delayed Feedback control method is employed to suppress those bifurcations, which lead to loss of stability of the desired rotational motion. First, the nonlinear dynamic analysis is carried out numerically for the system without control. Specifically, bifurcation diagrams and basins of attractions are computed showing co-existence of oscillatory and rotary attractors. Then numerical bifurcation diagrams are experimentally validated for a typical set of the system parameters giving undesired bifurcations. Finally, the control has been implemented and investigated both numerically and experimentally showing a good qualitative agreement.

Keywords

Parametric Pendulum, Time-Delayed Feedback method, Bifurcation control, Experimental dynamics

Introduction

Chaos control may be understood as the use of small perturbations in order to stabilise unstable periodic orbits (UPOs) embedded in chaotic attractors. Typically, it is a two-stage procedure including learning stage and control stage. Since unstable periodic orbits belong to the system dynamics, the stabilisation of these orbits is associated with low energy consumption. Therefore, this procedure is useful for different applications being of special interest to design flexible systems.

Chaos control methods may be split into discrete and continuous approaches. The essential ideas of these methods were proposed by the pioneer work of Ott et al. (1990), called OGY approach. This method is classified as discrete since it performs actuation in Poincaré sections (Ditto et al. 1995; Shinbrot et al. 1993). Semi-continuous method improved the applicability of the classical discrete methods presenting better performance for system with high instability. In general, multiparameter semicontinuous method can be understood as a generalization of the discrete methods (De Paula and Savi 2008, 2009). Continuous methods constitute an alternative to perform chaos control tending to be more robust. Several review articles can be found and they focus on the main ideas and techniques employed for chaos control in different applications. For example, Ogorzalek (1994); Arecchi et al. (1998); Fradkov and Evans (2002) presented reviews that furnish a general overview of chaos control methods, including discrete and continuous techniques. Pyragas (2006) gave an overview of continuous chaos control methods based on Time-Delayed Feedback. Boccaletti et al. (2000) treated tracking and synchronization of chaotic systems, mentioning several experimental implementations. Andrievskii and Fradkov (2003) discussed several methods

[1]Department of Mechanical Engineering Universidade de Brasília 70.910.900 - Brasília - DF - Brazil
[2]COPPE - Department of Mechanical Engineering Universidade Federal do Rio de Janeiro 21.941.972 - Rio de Janeiro - RJ, Brazil, P.O. Box 68.503
[3]Centre for Applied Dynamics Research, School of Engineering, University of Aberdeen, Aberdeen AB24 3UE, UK

Corresponding author:
Marian Wiercigroch, Centre for Applied Dynamics Research, School of Engineering, University of Aberdeen, Aberdeen AB24 3UE, UK.
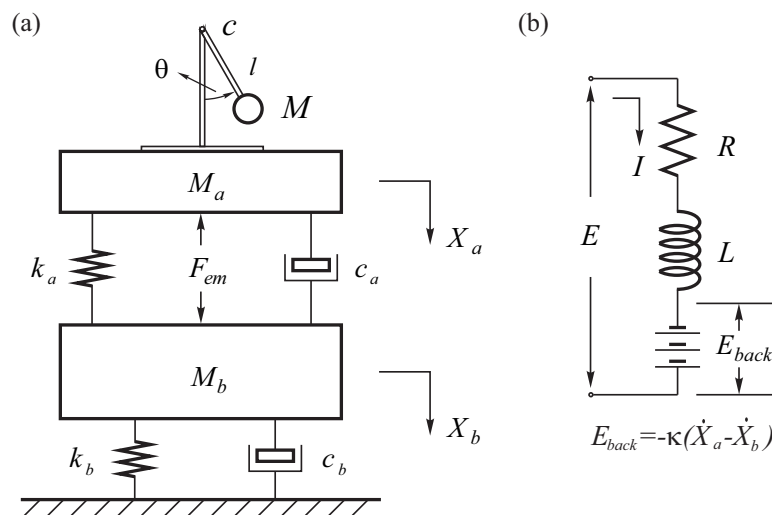Email: m.wiercigroch@abdn.ac.uk

Prepared using **sagej.cls** *[Version: 2013/07/26 v1.00]*

Figure 1. Physical model of the pendulum-shaker system with mechanical and electrical components. Adopted from Xu et al. (2007).

for controlling chaotic systems including chaos control techniques and traditional control methods, while Andrievskii and Fradkov (2004) mentioned several works that apply these control procedures to numerous systems of different fields. Fradkov et al. (2006) and Savi et al. (2006) presented reviews focused on chaos control methods applied to mechanical systems. Kapitaniak (1995) discussed the use of chaos control to synchronize dynamical systems. The synchronized rotation of pendulum then is studied extensively by Kapitaniak et al. (2014) and synchronization of pendulums systems is considered by Kapitaniak et al. (2015). De Paula and Savi (2011) presented a comparative analysis of chaos control methods discussing discrete, semi-continuous and continuous approaches.

The application of chaos control methods includes distinct subjects varying from aerospace to biomedical situations. But this idea is even more applicable by considering bifurcation control purposes. Specifically, the bifurcation control is of interest in structural stability where undesired system bifurcations may lead to the system stability loss. Nowadays, there is the comprehension that system failure is associated with eroded basins of attraction. Therefore, safe practical applications need to be related to uncorrupted basins. Under this assumption, several studies have been conducted under the name of dynamical integrity (Rega and Lenci 2009, 2005; Rega and Alaggio 2009; Lenci and Rega 2004; Gonçalves et al. 2011; Orlando et al. 2011), and bifurcation control is an interesting alternative to avoid instability issues.

De Paula et al. (2012) employed chaos control approach in order to perform bifurcation control in a parametrically excited pendulum. This pendulum application is related to the energy harvesting from sea waves and its main objective is to exploit the rotating solutions that exist over limited parameters range. This system has a lot of bifurcations that destabilize this kind of motion. In this regard, the bifurcation control can be useful in preserving the desired rotational solutions. The mentioned contribution has shown, using numerical analysis, that delayed feedback control methods can be successfully employed either to avoid bifurcations or to stabilise unstable periodic orbits.

This contribution revisits the bifurcation control of parametrically excited pendulum, dealing with both numerical and experimental points of view. A delayed feedback control method is employed in order to control bifurcations. Experimental results confirm the feasibility of the use of chaos control approach for bifurcation control. The analysis establishes a qualitative comparison between experimental and numerical results, presenting a good agreement. Moreover, this paper addresses the issue of limited availability of experimental results in the literature concerning chaos control methods applications, especially in mechanical systems.

Pendulum-shaker system

To study bifurcation control, we considered a parametric pendulum excited by electro-dynamical shaker which was previously analysed by Xu et al. (2007); Horton et al. (2008); Vaziri et al. (2014); Najdecka et al. (2015). Teh et al. (2015) investigated a similar system using RLC-circuit-powered solenoid. This pendulum system is considered here as a reference case which allows us to demonstrate the application of the bifurcation control methods both numerically and experimentally.

Figure 1 presents a schematics of the pendulum system showing mechanical and electrical parts. The mechanical system (Figure 1(a)) is comprised of three masses: the pendulum mass, M, the armature assembly mass, M_a, and the body mass, M_b, that represents the mass of the magnetic structure containing the field coil. The excitation is provided by an axial electromagnetic force, F_{em}, which is generated by the alternating current in the constant magnetic field represented by the electrical system (Figure 1(b)). The mechanical part of the pendulum-shaker system is described by three generalized
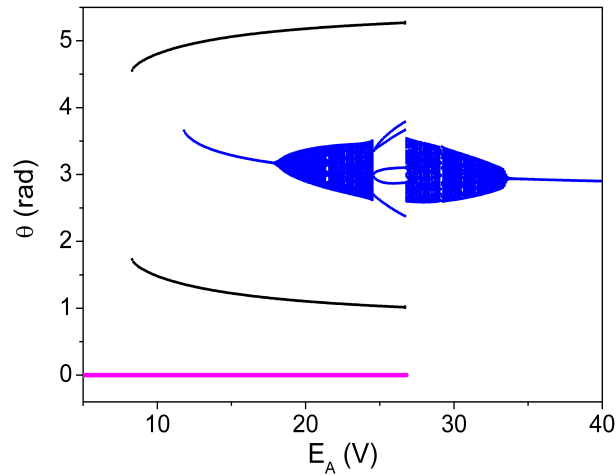

Figure 2. (colour online) Bifurcation diagrams for varying supplied voltage constructed at ω=1.51 Hz. The co-existing solutions are shown as period one rotating solution (and it's bifurcations) in blue, period two oscillating solution in black and pendulum at rest in pink.

coordinates: angular displacement of the pendulum, θ, and the vertical displacements of the body and the armature, X_b and X_a, respectively. The electrical system is described by the electric charge q, that is related to the current I by its derivative: $I = dq/dt$. Equations of motion of the parametric pendulum-shaker system are given below

$$
\begin{aligned}
Ml\ddot{\theta} + cl\dot{\theta} &+ \frac{2}{\pi}F_\mu \tan^{-1}(\alpha\,\dot{\theta}) + Mg\sin\theta = \\
&M\ddot{X}_a \sin\theta, \\
(M_a + M)\ddot{X}_a &+ c_a(\dot{X}_a - \dot{X}_b) + k_a(X_a - X_b) = \\
&(M_a + M)g + Ml\,\ddot{\theta}\sin\theta + Ml\,\dot{\theta}^2\cos\theta - \kappa I, \\
M_b\ddot{X}_b &+ c_b\dot{X}_b - c_a(\dot{X}_a - \dot{X}_b) + k_bX_b \\
&- k_a(X_a - X_b) = M_bg + \kappa I, \\
R_E I &+ L\frac{dI}{dt} - \kappa(\dot{X}_a - \dot{X}_b) = \\
&E_A\cos(\Omega\,t)
\end{aligned}
\tag{1}
$$

where F_μ is the torque due to dry friction. Equations of motion are based on the formulation proposed by Xu et al. (2007) adding terms related to dry friction (for more details see De Paula et al. 2006).

Table 1. Experimentally determined parameters of the pendulum-shaker system.

Name	Description	Value	Name	Description	Value
M	mass of the pendulum	0.709 kg	l	length of the pendulum	0.2605 m
c	damping coefficient of pendulum	0.0828 kg/s	M_a	mass of armature assembly	27.58 kg
k_a	first stiffness	86175.9 kg/s^2	c_b	damping coefficient of shaker body	679.35 kg/s
M_b	mass of body (magnetic structure)	820 kg	k_b	second stiffness	244284 kg/s^2
c_a	damping coefficient of shaker armature	534.05 kg/s	κ	coupling coefficient between electro-magnetic force and current	130 N/A
L	coil inductance	2.626 $\times 10^{-3}$ H	R_E	coil resistance	0.3 Ω
F_μ	torque due to dry friction	0.0625 Nm	α	constant	10^6

Considering the state variables $\{x_1, x_2, x_3, x_4, x_5, x_6, x_7\} = \{\theta, \dot{\theta}, X_a, \dot{X}_a, X_b, \dot{X}_b, I\}$, the equations of motion are now written as a set of first order differential equations:

$$\dot{x}_1 = x_2,$$

$$\dot{x}_2 = [(-\frac{2}{\pi}F_\mu \tan^{-1}(\alpha x_2) - clx_2)(M_a + M) - [c_a(x_4 - x_6)$$
$$+ k_a(x_3 - x_5) + \kappa x_7]M\sin x_1 + M^2 l x_2^2 \cos x_1 \sin x_1]$$
$$/[Ml(M_a + M - M\sin^2 x_1)] + \frac{T_C}{Ml},$$

$$\dot{x}_3 = x_4,$$

$$\dot{x}_4 = [(M_a + M)g + Mlx_2^2 \cos x_1 - \kappa x_7 - c_a(x_4 - x_6)$$
$$- k_a(x_3 - x_5) - (clx_2 + \frac{2}{\pi}F_\mu \tan^{-1}(\alpha x_2))\sin x_1$$
$$- mg\sin^2 x_1]/[M_a + M - M\sin^2 x_1],$$

$$\dot{x}_5 = x_6,$$

$$\dot{x}_6 = [M_b g + \kappa x_7 - c_b x_6 + c_a(x_4 - x_6) - k_b x_5$$
$$+ k_a(x_3 - x_5)]/M_b,$$

$$\dot{x}_7 = [E_A\cos(\Omega t) - R_E x_7 + \kappa(x_4 - x_6)]/L.$$

(2)

where T_C is added, which corresponds to the control parameter actuation and consists of a torque applied to the pendulum. Xu et al. (2007) discussed experimental aspects of the pendulum-shaker dynamics and the system parameter identification procedure. Thus the shaker system parameters obtained in Xu et al. (2007) are employed in this work and they are presented in Table 1 together with some new parameters related to the pendulum rig. Numerical simulations are performed using Eq. 1 and parameters presented in Table 1.

Initially, the uncontrolled behaviour of the system is considered. It is noticeable that for ω =1.51 Hz and a range of voltage, the pendulum presents a period-1 rotation behaviour. This type of response among other rotational responses are important for energy harvesting purposes (Najdecka 2013). Therefore, it is interesting to investigate the bifurcation possibilities from this desired solution. Bifurcation diagrams are constructed by considering the stroboscopic sampled angular displacement against the slow quasi-static variation of the voltage, which is directly related to the forcing amplitude. During voltage decrease, the last state of the previous voltage value is employed as initial condition for the next value. Therefore, if there are a number of coexisting solutions, it is possible to alter the bifurcation diagram by changing the decrement of voltage, as in this case the different voltage values will be picked up for calculations resulting also in variation of initial conditions. Figure 2 presents bifurcation diagrams constructed from the period-1 behaviour, decreasing the voltage values by different decrements. Note that different variations of the voltage supply lead to different initial conditions for each voltage, causing different behaviours of the system until the final stationary response is reached. All analysed cases are plotted together in Figure 2, where coexisting attractors can be observed, including quasi-periodic behaviour, period one, two and five orbits as well as the pendulum in rest.

Figure 3 presents one possibility related to the bifurcation diagrams shown in Figures 2 and shows system response details for some fixed values of E_A. In this case, for each supplied voltage value, system response is considered during 450
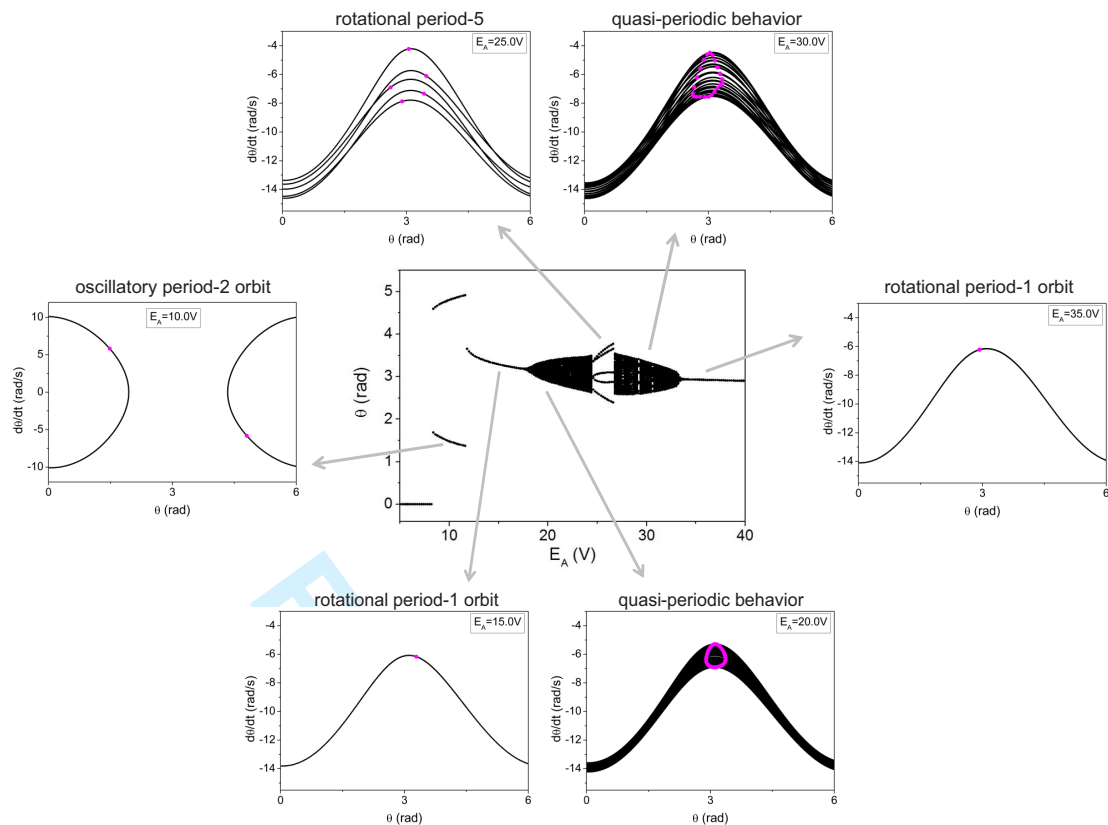
Figure 3. (colour online) The bifurcation diagram constructed at ω=1.51 Hz for varying supplied voltage and corresponding phase portraits unveiling the system behaviour. Period two oscillating solution is presented for $E_A = 10$ V and various rotating solutions are shown for higher values of the voltage $E_A = 15;\ 20;\ 30$ and 35 V.

forcing periods and the first 350 forcing periods are eliminated as transient. The voltage variation here is $\triangle E_A$=-0.1 V. This bifurcation diagram was chosen as it contains all response possibilities observed in Figure 2. Figure 3 presents phase portraits together with Poincaré section of rotational period-1, oscillatory period-2 and rotational period-5 orbits and quasi-periodic behavior at correspondent supplied voltage. As can be seen from this Figure, rotation period-1 solution is observed in the voltage range of [11.73, 17.60] V and [33.47, 40] V, the oscillatory period-2 solution is seen at [8.32, 11.73] V, rotational period-5 solution at [24.50, 26.72] V and and quasi-periodic behaviour is seen at [17.60, 24.50] V and [26.72, 33.47] V. Also the pendulum at rest is recorded for voltage range of [4, 8.32] V.

Figure 2 shows a multi-stable behaviour of the system demonstrating coexisting attractors at the selected supplied voltages. To explore those attractors in more details, their basins of attractions are considered next. Figure 4(a) presents the basins of attraction for ω=1.51 Hz and E_A=25 V. In this case, three co-existing responses are observed: period-2 oscillatory motion (pink basin), period-5 orbit (dark blue basin) and the pendulum in stationary response (light blue basin). The period-5 orbit is the same as presented in Figure 3 while the period-2 oscillatory motion is similar to the one shown in Figure 3 for $E_A = 10$ V. Figure 4(b) presents the basin of attraction for ω=1.51 Hz and E_A=22.5 V. In this case, a quasi-periodic behaviour (black basin) appears, as well as the period-2 oscillatory motion and the pendulum in stationary response, however, period-5 orbit is not observed anymore. It is important to note that in Figure 4(b) black points (related to quasi-periodic response) appear instead of dark blue points (related to period-5 response). Note that system dimension is 7, thus, basins of attraction presented in Figure 4 only give sections of the basins on pendulum angle and rotational velocity plane. The initial conditions of all other state variables are considered equal to zero.

The next section considers experimental data of the uncontrolled system, establishing a comparison with numerical results.

Numerical and experimental analysis of the uncontrolled system

Experimental analysis of the pendulum system has been carried out using an experimental set up available in the Centre of Applied Dynamics Research at the University of Aberdeen. The setup consists of a pendulum rig fixed to an electromechanical shaker as shown in Figure 5 and have inspired the rig described in Yokoi & Hikihara (Yokoi and Hikihara
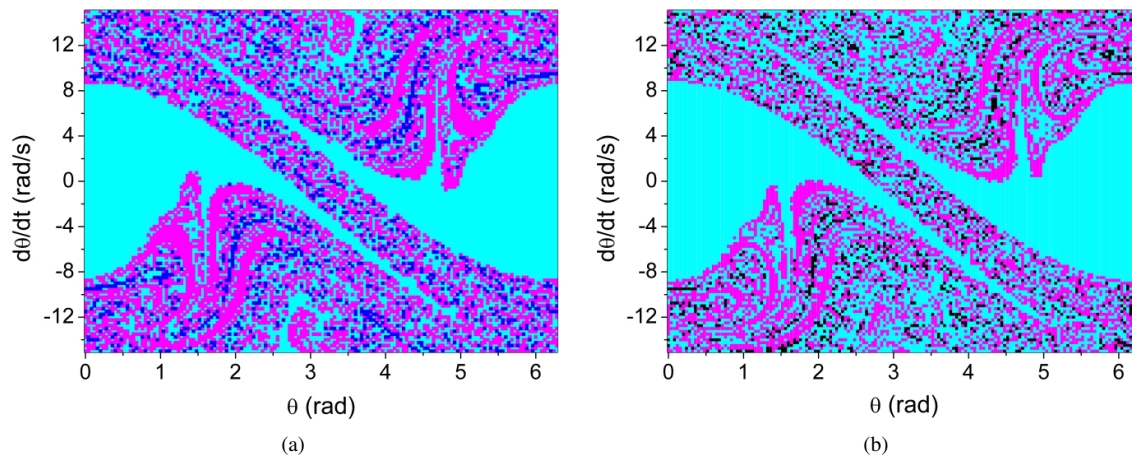
Figure 4. (colour online) Basins of attraction for ω=1.51 Hz. (a) E_A=25 V; (b) E_A=22.5 V. The basin of the period two oscillatory solution is shown in light blue, the basin of the stationary (rest) solution is in pink and the dark blue basin in part (a) corresponds to period five rotating solution whereas the black basin in part (b) is of quasi-periodic rotating solution.

2011). A shaker provides the harmonic excitation of the system and two independent pendulums, with adjustable length and bob masses at the ends, are threaded to pendulum rods on the common supporting base. The rod is attached to a shaft, supported by needle bearing, in order to minimize friction. The shaft has a gear with a belt that provides the coupling to a low inertia DC servo-motor of 1600rpm, which actuates over the system. A three channel hollow shaft encoder with 500ppr monitors the angular position of the pendulum. An accelerometer is fixed on the base of whole rig in order to measure the actual excitation. Basically, it is a vertically parametric excited pendulum, similar to the one considered in De Paula et al. (2012). In the study presented in this paper, only one pendulum is used, the other one is kept immovable.

A NI PCI-6251 card and Labview software are employed for data acquisition, providing output signal for real-time control. In order to minimize real-time calculations in the Labview code, a converter provides the connection between the encoder and the PCI-6251, which transform digital signal from encoder to continuous angle displacement.

The comparison between numerical and experimental results needs to consider an important difference in terms of system parameter. Numerical model has a voltage E_A that represents the voltage supplied to the shaker, which is directly related to the forcing amplitude. This voltage is a consequence of an amplification of the voltage E_0 that is supplied to an amplifier in experimental set up. In the proposed experimental apparatus, E_0 is the measured variable. This signal represents an input to
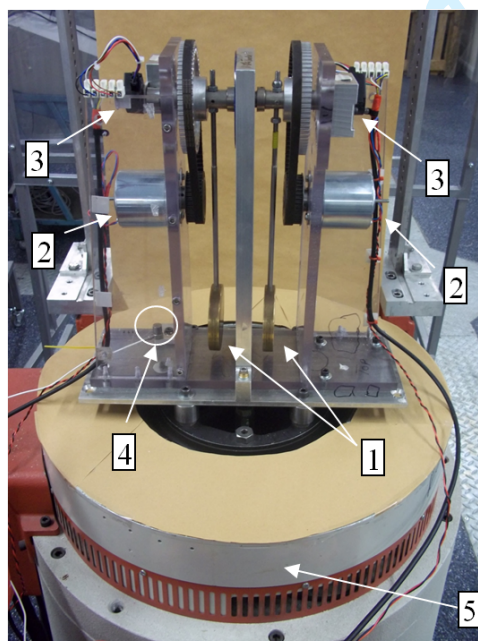

Figure 5. (colour online) Experimental rig: (1) independent pendula; (2) servo motors; (3) encoders; (4) accelerometer; (5) shaker.
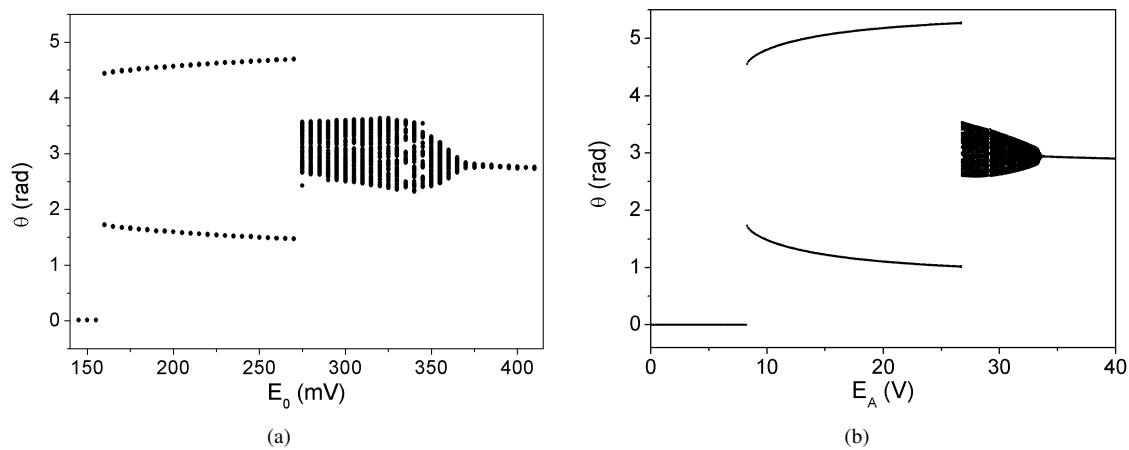
Figure 6. Bifurcation diagram of the uncontrolled system constructed at ω=1.51 Hz for decreasing forcing amplitude. (a) experimental results; (b) numerical simulations.

an amplifier that output is the input voltage of the shaker, E_A. Since our measurements actually record E_0, these values are presented in all results, and they are different from the values of E_A used in numerical simulations. Due to some technical limitations of the experimental equipment used, it was not possible to record the amplified signal supplied to the shaker, E_A. However the comparisons between the experimental and numerical results allows to estimate the amplification factor as approximately 7950 (i.e. $E_A = 7946.40 \cdot E_0 + 85.27$).

The experimental bifurcation diagram is constructed in the same way as the numerical one, by considering the stroboscopic sampled angular displacement of the pendulum against the slow quasi-static variation of the voltage. From an initial forcing amplitude with ω=1.51 Hz, where the pendulum presents a period-1 rotation behaviour, a decrease of the voltage supply is performed. Figure 6(a) shows bifurcation diagram experimentally obtained, while Figure 6(b) presents the correspondent numerical bifurcation diagram, which corresponds to one of the situations presented in Figure 2. Note the good agreement between both results presenting the same qualitative behaviours for the whole range of parameters.

In the case of the experimental diagram, the plot starts with an E_0=410 mV, decreasing till E_0=140 mV that is reached by increments $\triangle E_0$=-5 mV in the supplied voltage. For higher voltages, which correspond to higher forcing amplitude, rotational period-1 response is observed. As the voltage supply decreases, there is a bifurcation to a quasi-periodic response which includes a small periodic window close to E_0=335 mV. For lower voltage, with values close to 270 mV, a bifurcation occurs leading to an oscillatory period-2 behaviour. Finally, for smaller voltage supply, the pendulum stops presenting a stationary response.

The general behaviour of the pendulum system is treated in more details by considering phase space and Poincaré sections. Figure 7 presents pendulum dynamics experimentally obtained for ω=1.51 Hz and different values of supplied voltage, highlighting the behaviours presented in the bifurcation diagram. Basically, six different values of E_0 are shown: 400, 360, 340, 335, 295, 270 mV. Note that the period-1 rotation solution for E_0= 400 mV changes to quasi-periodic solutions when E_0= 360 mV, E_0= 340 mV and E_0= 295 mV. Inside this region, it is important to observe a periodic response when E_0=335 mV. Finally, the system presents a period-2 response when E_0=270 mV. Figure 8 presents the same results obtained by numerical simulations. Note the good qualitative agreement between them.

Our control aim is to avoid non-rotational behaviours, forcing the system to keep the period-1 rotational orbit. This can be achieved with chaos control approach (De Paula et al. 2012; Yokoi and Hikihara 2011). The next section deals with system control by considering numerical and experimental approaches, and the goal is to avoid bifurcations that destabilize the desired period-1 rotational orbit.

Numerical and experimental bifurcation control

Chaos control methods can be split into discrete and continuous methods. Continuous methods are based on Time-Delayed Feedback control that performs continuous-time perturbations to achieve stabilisation. This approach was first proposed by Pyragas (1992) and deals with a dynamical system modelled by a set of ordinary nonlinear differential equations as follows:
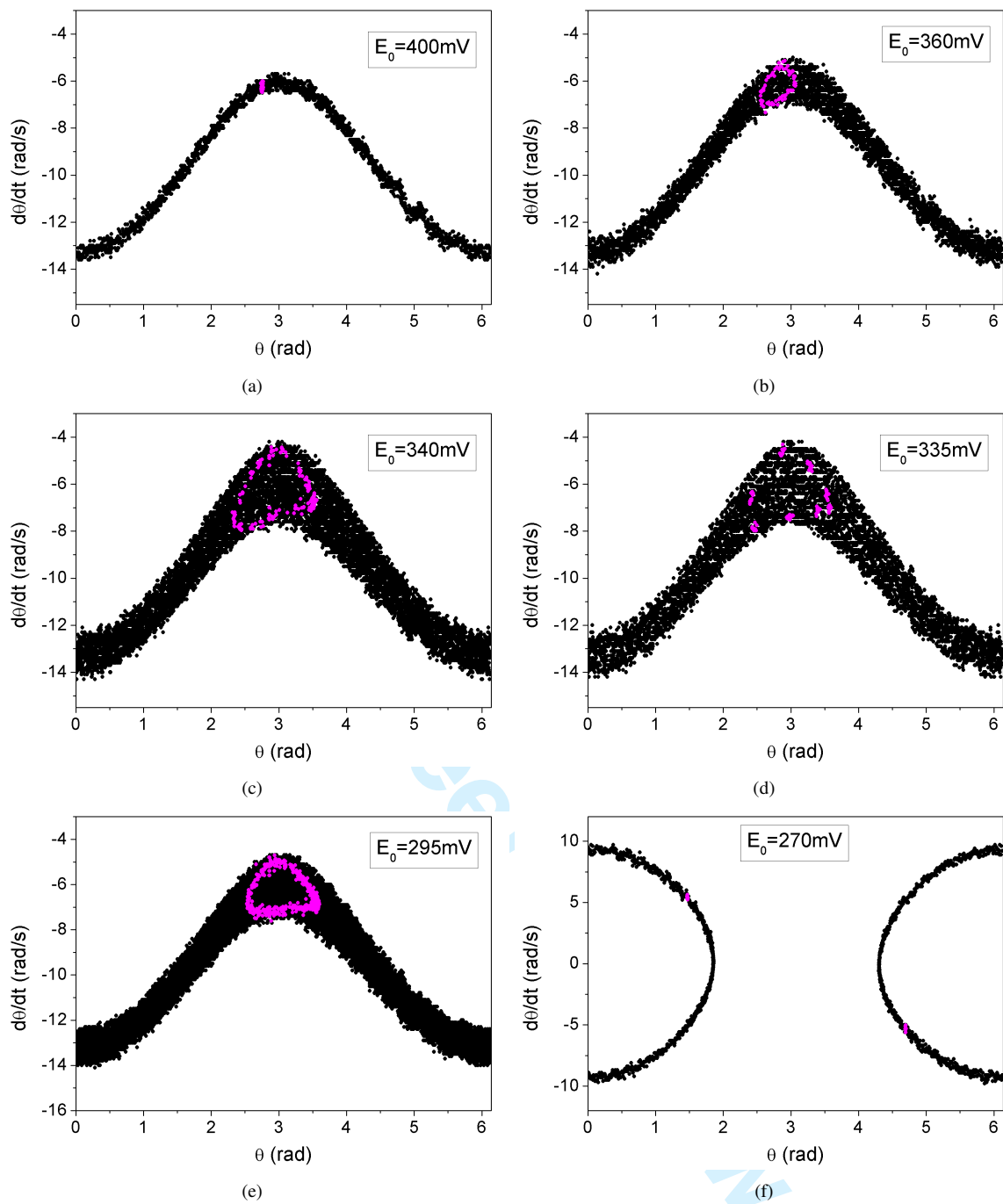
Figure 7. (colour online) Phase portraits (in black) together with Poincaré sections (in pink) for ω=1.51 Hz and different supplied voltage E_0 obtained experimentally. Parts (a)–(e) demonstrate various rotating solutions while part (f) present period two oscillating response.

$$\dot{\mathbf{x}}(t) = \mathbf{Q}(\mathbf{x}, t) + \mathbf{B}(\mathbf{x}, t) \tag{3}$$

where t is time, $\mathbf{x}(t) \in \Re^n$ is the state variable vector, $\mathbf{Q}(\mathbf{x}, t) \in \Re^n$ defines the system dynamics, while $\mathbf{B}(\mathbf{x}, t) \in \Re^n$ is associated with the control action. Pyragas (1992) proposed a control law named Time-Delayed Feedback control (TDF) considering the information of time-delayed states of the system represented by the following equations:

$$\mathbf{B}(\mathbf{x}, t) = \mathbf{K} \left[\mathbf{x}_\tau - \mathbf{x} \right] \tag{4}$$

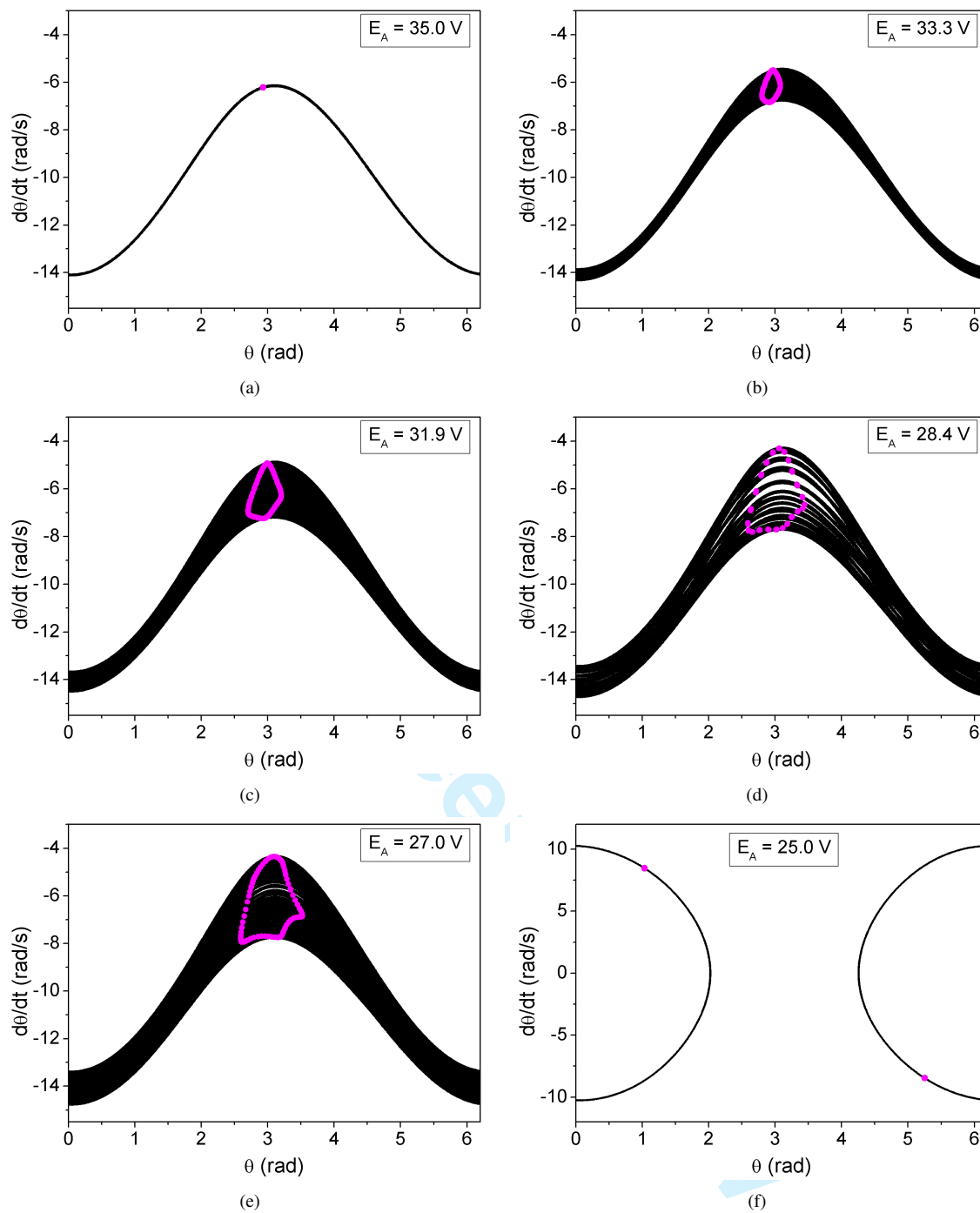**Figure 8.** (colour online) Phase portraits (in black) together with Poincaré sections (in pink) for ω=1.51 Hz and different supplied voltage E_A obtained numerically. Parts (a)–(e) demonstrate various rotating solutions while part (f) present period two oscillating response.

where $\mathbf{K} \in \Re^{n \times n}$ is the feedback gain matrix, $\mathbf{x}_\tau = \mathbf{x}(t - \tau)$ is a delayed state of the system and τ is the time delay. The UPO stabilisation can be achieved by an appropriate choice of $\mathbf{K}$. Note that for any gain defined by $\mathbf{K}$, perturbation of Eq. 2 vanishes when the system is on the UPO since $\mathbf{x}(t - \tau) = \mathbf{x}(t)$ if $\tau = T_i$, where T_i is the periodicity of the ith UPO.

The mechanical state variables related to the pendulum are the angular position, $x_1 = \theta$, and angular velocity, $x_2 = \dot{\theta}$. An encoder is employed to monitor the position x_1, and therefore, it is considered as an observed variable.

The control action, $\mathbf{B}(x, t)$, is represented by an scalar variable, $B_2(x_1, t) = B(x_1, t)$, as follows:

$$B(x_1, t) = K\left[x_1(t - \tau) - x_1(t)\right] \tag{5}$$

where τ is the periodicity of the orbit to be stabilised. Since the main goal of this controller is to preserve a rotational behaviour, the UPO to be stabilised is always a period-1 response, and therefore, $\tau = 2\pi/\omega$. Note that, since angular position is employed in the control law, only component K_{21} of Eq. 4 is different from zero.

De Paula et al. (2012) employed a similar control procedure where the control action was only applied to one differential equation, the one related to time evolution of the angular velocity. In the cited article the control law was associated with delayed and actual values of angular velocity, and only component K_{22} of Eq.3 was different from zero. On the other hand, this work considers that the applied torque is proportional to the difference between a delayed and the actual pendulum angular position since this is the observed variable in the experiment, obtained by the encoder. To use pendulum velocity instead of its position in control law, the obtained displacement has to be numerically derived, what introduces errors. Another difference related to both controllers is related to the control law. The previous reference employed the Extended Time-Delayed Feedback control (ETDF), proposed by Socolar et al. (1994), that considers several delayed states instead of only one considered in the TDF.

By using the formalism presented for the Time-Delayed Feedback control law and Eq.2, the control actuation TC may be expressed as follows:

$$T_C = Ml \ K[x_1(t - \tau) - x_1(t)]. \tag{6}$$

In order to perform the control of the system it is necessary to determine control gain, K. An interesting approach is the use of Lyapunov exponents associated with the desired period-1 rotational orbit. This orbit is identified just before the bifurcation to the quasi-periodic behaviour and its largest Lyapunov exponent is numerically calculated with the algorithm proposed by Wolf et al. (1994), as indicated in De Paula et al. (2012). Figure 9 presents results related to the maximum Lyapunov exponent of the period-1 orbit indicating the use of K=1 as a good alternative to perform control (Pyragas 1992; De Paula and Savi 2011). From now on, the controlled response is treated assuming $K = 1$. The forthcoming analysis exploits the idea of applying TDF method to avoid bifurcations that changes the desired periodic rotational orbit. Therefore, we will look now at a comparison between system responses with and without control action concentrating on the bifurcation control.

Initially, the case presented in Figure 6 (ω=1.51 Hz) is considered where there is a bifurcation from the period-1 response to a quasi-periodic response and then, to a period-2 behaviour. System behaviour with control action (in pink) is presented in the bifurcation diagram shown in Figure 10 together with uncontrolled behaviour (in black). Figure 10(a) presents experimental results while Figure 10(b) shows numerical simulations. All points of Poincaré section are plotted, including transient response. Note that the controller eliminates the bifurcation, preserving the periodic rotational behaviour. Figure 11 shows experimental pendulum phase portrait when voltage supply is 320 mV, and Figure 12 presents the same situation for numerical results, when the voltage supply of the shaker is 30 V.

The robustness of the controller to perform bifurcation control can be observed by changing the steps of the decrease of the voltage supply. Hence, it is assumed the same conditions of the preceding simulation (ω=1.51 Hz, K=1), but the
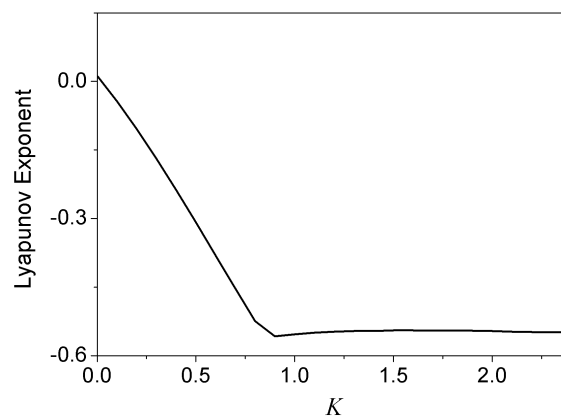

Figure 9. Largest Lyapunov exponent of period-1 rotational orbit for different control gain, K.
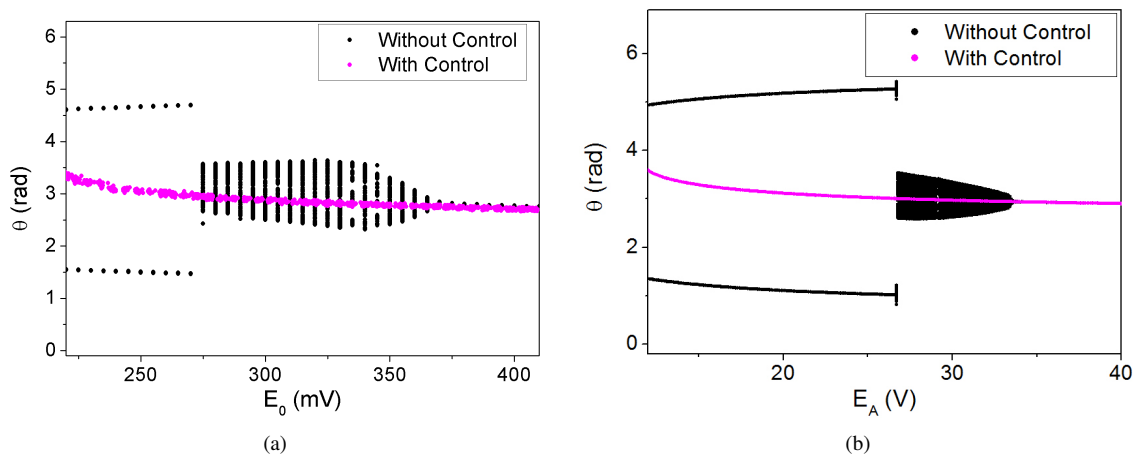
Figure 10. (colour online) (a) experimental and (b) numerical bifurcation diagrams without and with control action for $K=1$ and $\omega=1.51$ Hz.

voltage supply steps are changed. Figure 13 presents two different experimental results with $\triangle E_0$=-10 mV and $\triangle E_0$=-20 mV, showing that the controller successfully control bifurcations. Note that the change in voltage steps does not alter the stabilisation procedure.

The robustness of the controller was also checked by varying the initial control application orbit. The pendulum was set to oscillate with $\omega=1.51$ Hz and the voltage supply was decreased until quasi-periodic behaviour occurred without control. Then, when the voltage was close to the bifurcation that leads to period-2 oscillatory orbit, the control was turned on, using $K=1$. Experimental approach considers $\triangle E_0$=-10 mV. Figure 14 presents the bifurcation diagram for this situation showing that the controller is able to reach the desired period-1 rotational solution, even starting from a different condition. Figure 14(a) shows experimental results while Figure 14(b) presents numerical simulations. Figure 15 presents stabilisation details of the experimental approach when the control action starts from the quasi-periodic behaviour, while Figure 16 presents the same results for the numerical simulation. Note that although the control method is continuous, the control action shown in Figure 15(b) presents also some spikes. It is important to mention that in this particular case, after the bifurcation to the quasi-periodic motion, the desired period one orbit becomes unstable. Therefore, the control action is only required to stabilize this orbit and as in general case of control of UPOs, the control action is rather small. Once the orbit was stabilised, the control action is required only when the supplied voltage is varied and due to noise. These small perturbations combined with the minimum actuation provided to the DC servo-motor (±20 mV) and the frequency sampling lead to the presented spikes in control action as time increases.

We turn our attention now to the control by considering experimental results of Figures 11 and 15, and numerical simulations shown in Figures 12 and 16. Here we obtained that the control effort to stabilise the rotational orbit is larger
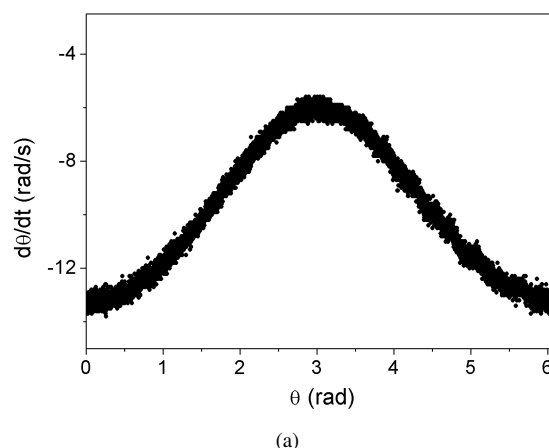

Figure 11. Phase portrait of the stabilised rotational orbit obtained experimentally under control action for E_0=320 mV.
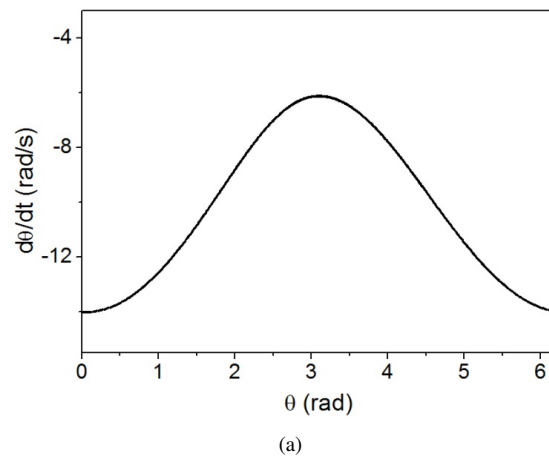
(a)

Figure 12. Phase portrait of the stabilised rotational orbit obtained numerically under control action for E_A=30 V.
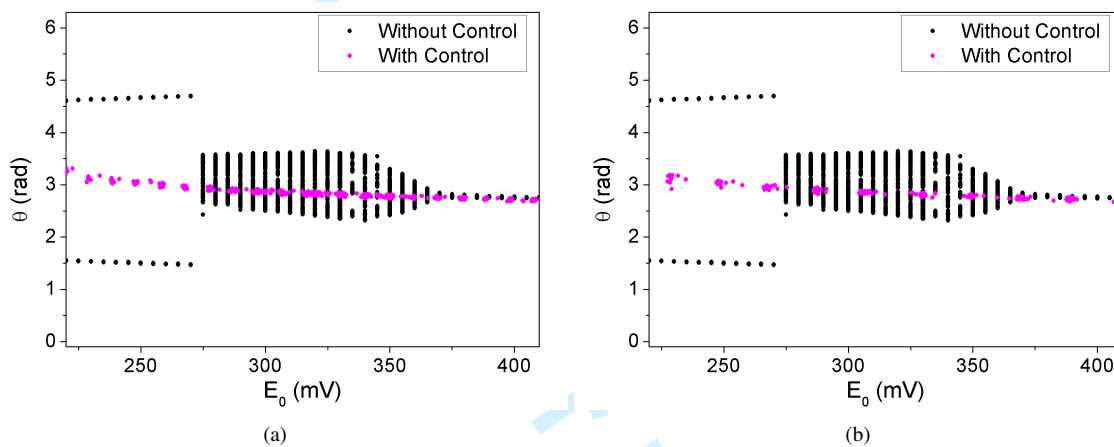

(a)   (b)

Figure 13. (colour online) Bifurcation diagrams without and with control action for K=1, ω=1.51 Hz and two different voltage supply variations: (a) $\triangle E_0$=-10 mV and (b) $\triangle E_0$=-20 mV.
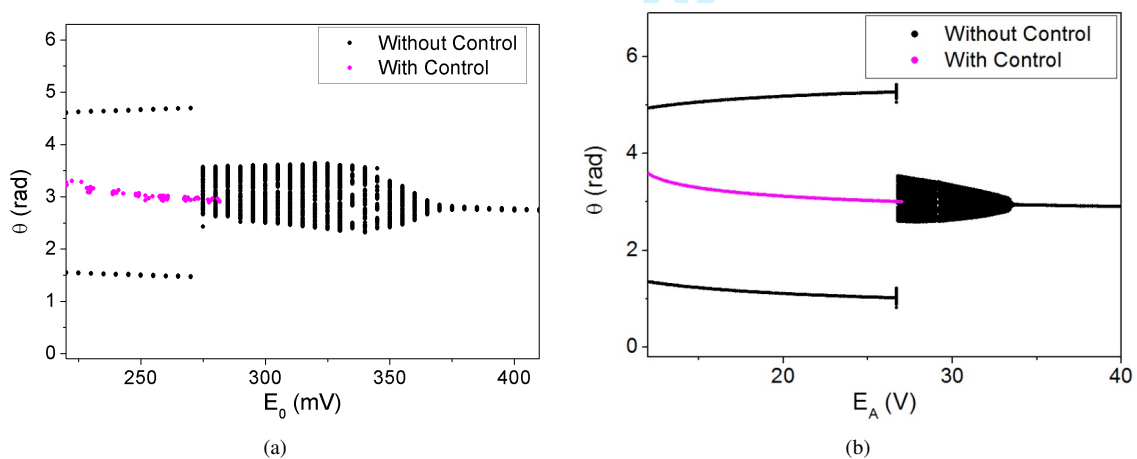

(a)   (b)

Figure 14. (colour online) (a) experimental and (b) numerical bifurcation diagrams without and with control action starting from quasi-periodic behaviour for K=1 and ω=1.51 Hz.

when control action starts at a quasi-periodic response. Besides, it is important to observe that, once stabilised, the control effort decreases. In numerical situation, without noise, the control effort vanishes after the orbit stabilisation. On the other hand, experimental control, with unavoidable noise, the control action works to compensate noise influence.

De Paula et al. (2012) discussed the numerical application of the chaos control approach in different situations: classical chaos control is applied stabilising some UPOs embedded in chaotic attractor; period doubling bifurcation is prevented preserving a period-1 rotating orbit; bifurcation to chaos is avoided preserving a stable rotating solution. Here,
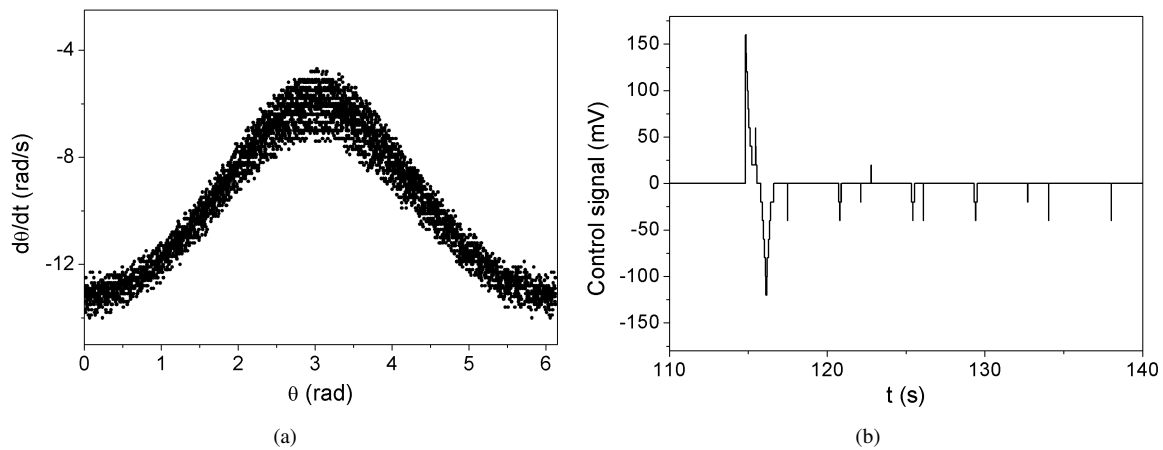
Figure 15. Stabilisation details of experimental control for control starts from a quasi-periodic behaviour. (a) phase portrait; (b) control action.
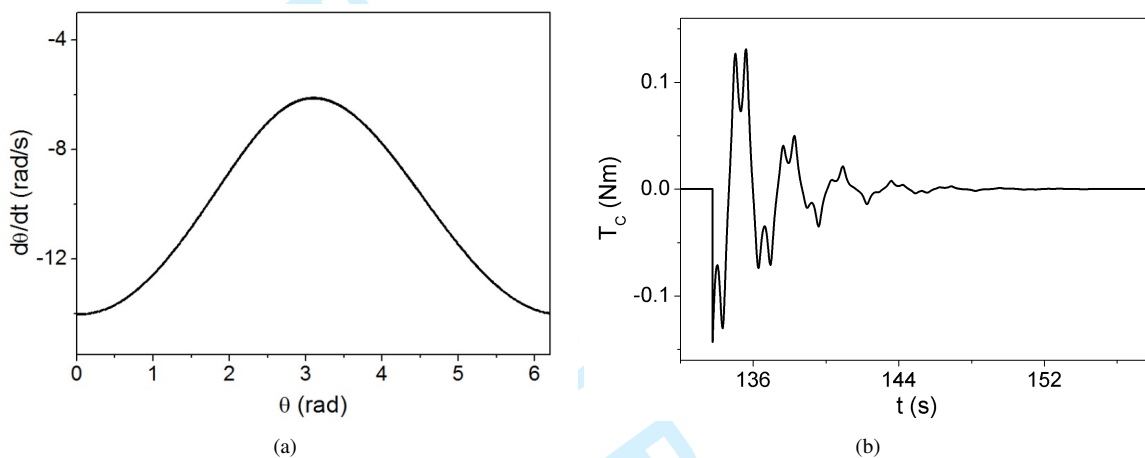

Figure 16. Stabilisation details of numerical control for control starts from a quasi-periodic behaviour. (a) phase portrait; (b) control action.

an experimental confirmation of some of these results is obtained by showing the bifurcation control. All experimental results are accompanied to numerical results showing a good qualitative agreement.

Conclusions

This contribution deals with the application of chaos control methods to perform numerical and experimental bifurcation control of a parametrically excited pendulum driven by an electro-dynamical shaker. Bifurcation diagrams are constructed for the supplied voltage variations showing bifurcation from the desired rotational solution to quasi-periodic and oscillatory period-2 responses.

The delayed feedback control is successfully employed to avoid bifurcation that destabilise the desired period-1 rotational orbit. Experimental and numerical results present a good qualitative agreement showing the capability of the chaos control approach for bifurcation control purposes.

References

Andrievskii B and Fradkov A (2003) Control of chaos: Methods and applications. I: Methods. Automation and Remote Control 64(5): 673–713.

Andrievskii B and Fradkov A (2004) Control of chaos: Methods and applications. II: Applications. Automation and Remote Control 65(4): 505–533.

Arecchi F, Boccaletti S, Ciofini M, Meucci R and Grebogi C (1998) The control of chaos: theoretical schemes and experimental realizations. International Journal of Bifurcation and Chaos 8(08): 1643–1655.

Boccaletti S, Grebogi C, Lai YC, Mancini H and Maza D (2000) The control of chaos: theory and applications. Physics Reports 329(3): 103–197.

De Paula A and Savi M (2008) A multiparameter chaos control method applied to maps. Brazilian Journal of Physics 38(4): 536–542.

De Paula A and Savi M (2009) A multiparameter chaos control method based on OGY approach. Chaos, Solitons and Fractals 40(3): 1376–1390.

De Paula A and Savi M (2011) Comparative analysis of chaos control methods: A mechanical system case study. International Journal of Non-Linear Mechanics 46(8): 1076–1089.

De Paula A, Savi M and Pereira-Pinto F (2006) Chaos and transient chaos in an experimental nonlinear pendulum. Journal of Sound and Vibration 294: 585–595.

De Paula A, Savi M, Wiercigroch M and Pavlovskaia E (2012) Bifurcation control of a parametric pendulum. International Journal of Bifurcation and Chaos 22(05): 1250111.

Ditto W, Spano M and Lindner J (1995) Techniques for the control of chaos. Physica D 86: 198–211.

Fradkov A and Evans R (2002) Control of chaos: survey 1997-2000. In: World Congress, volume 15. pp. 1643–1643.

Fradkov A, Evans R and Andrievsky B (2006) Control of chaos: methods and applications in mechanics. Philosophical Transactions of the Royal Society A 364: 2279–2307.

Gonçalves P, Silva F, Rega G and Lenci S (2011) Global dynamics and integrity of a two-dof model of a parametrically excited cylindrical shell. Nonlinear Dynamics 68: 117–128.

Horton B, Wiercigroch M and Xu X (2008) Transient tumbling chaos and damping identification for parametric pendulum. Philosophical Transactions of the Royal Society A: Mathematical, Physical and Engineering Sciences 366(1866): 767–784.

Kapitaniak M, Czolczynski K, Perlikowski P, Stefanski A and Kapitaniak T (2014) Synchronous states of slowly rotating pendula. Physics Reports 541(1): 1–44.

Kapitaniak M, Lazarek M, Nielaczny M, Czolczynski K, Perlikowski P and Kapitaniak T (2015) Synchronization extends the life time of the desired behavior of globally coupled systems. Scientific Reports 4: 4391.

Kapitaniak T (1995) Continuous control and synchronization in chaotic systems. Chaos Solitons & Fractals 6: 237–244.

Lenci S and Rega G (2004) A unified control framework of the non-regular dynamics of mechanical oscillators. Journal of Sound and Vibration 278: 1051–1080.

Najdecka A (2013) Rotating dynamics of pendula systems for energy harvesting from ambient vibrations. PhD Thesis, University of Aberdeen, UK.

Najdecka A, Kapitaniak T and Wiercigroch M (2015) Synchronous rotational motion of parametric pendulums. International Journal of Non-Linear Mechanics 70(0): 84–94.

Ogorzalek M (1994) Chaos control: how to avoid chaos or take advantage if it. Journal of the Franklin Institute 331B(6): 681–704.

Orlando D, Goncalves P, Rega G and Lenci S (2011) Influence of modal coupling on the nonlinear dynamics of Augusti's model. Journal of Computational and Nonlinear Dynamics 6(4).

Ott E, Grebogi C and Yorke J (1990) Controlling chaos. Physical Review Letters 64(11): 1196–1199.

Pyragas K (1992) Continuous control of chaos by self-controlling feedback. Physics Letters A 170(6): 421–428.

Pyragas K (2006) Delayed feedback control of chaos. Phil. Trans. R. Soc. A 364: pp. 2309–2334.

Rega G and Alaggio R (2009) Experimental unfolding of the nonlinear dynamics of a cable-mass suspended system around a divergence-hopf bifurcation. Journal of Sound and Vibration 322: 581–611.

Rega G and Lenci S (2005) Identifying, evaluating, and controlling dynamical integrity measures in nonlinear mechanical oscillators. Nonlinear Analysis 63: 902–914.

Rega G and Lenci S (2009) Dynamical integrity and control of nonlinear mechanical oscillators. Journal of Sound and Vibration 14(1-2): 159–179.

Savi M, Pereira-Pinto, FHI and Ferreira A (2006) Chaos control in mechanical systems. Shock and Vibration 13: 301–314.

Shinbrot T, Grebogi C, Ott E and Yorke J (1993) Using small perturbations to control chaos. Nature 363: 3411–417.

Socolar J, Sukow D and Gauthier D (1994) Stabilizing unstable periodic orbits in fast dynamical systems. Physical Review.B, Condensed matter 50(4): 3245–3248.

Teh SH, Chan KH, Woo KC and Demrdash H (2015) Rotating a pendulum with an electromechanical excitation. International Journal of Non-Linear Mechanics 70(0): 73–83.

Vaziri V, Najdecka A and Wiercigroch M (2014) Experimental control for initiating and maintaining rotation of parametric pendulum. The European Physical Journal Special Topics 223(4): 795–812.

Wolf A, Swift J, Swinney H and Vastano J (1994) Determining lyapunov exponents from a time series. Physica D 16: 285–317.

Xu X, Pavlovskaia E, Wiercigroch M, Romeo F and Lenci S (2007) Dynamic interactions between parametric pendulum and electro-dynamical shaker. ZAMM Zeitschrift fur Angewandte Mathematik und Mechanik 87(2): 172–186.

Yokoi Y and Hikihara T (2011) Tolerance of start-up control of rotation in parametric pendulum by delayed feedback. Physics Letters, Section A: General, Atomic and Solid State Physics 375(17): 1779–1783.

Prepared using sagej.cls